Author Manuscript

Title: Simultaneous Control of Pore-Space Partition and Charge Distribution in Multi-Modular Metal-Organic Frameworks

Authors: Pingyun Feng, Prof. Dr.; Anh N. Hong; Emily Kusumoputro; Yanxiang Wang; Huajun Yang; Yichong Chen; Xianhui Bu

To be cited as: 10.1002/anie.202116064

Link to VoR: https://doi.org/10.1002/anie.202116064

COMMUNICATION

Simultaneous Control of Pore Space Partition and Charge Distribution in Multi-Modular Metal-Organic Frameworks

Anh N. Hong,[a] Emily Kusumoputro,[a] Yanxiang Wang,[a] Huajun Yang,[b] Yichong Chen,[a] Xianhui Bu,*[,b] Pingyun Feng*[,a]

[a] Anh N. Hong, Emily Kusumoputro, Yanxiang Wang, Yichong Chen, Prof. P. Feng
Department of Chemistry
University of California, Riverside, CA 92521
Email: pyfeng@ucr.edu
[b] Dr. H. Yang, Prof. X. Bu
Department of Chemistry and Biochemistry
California State University Long Beach
1250 Bellflower Boulevard, Long Beach, CA 90840
E-mail: xianhui.bu@csulb.edu

Supporting information for this article is given via a link at the end of the document.

Abstract: We report here a strategy for making anionic pacs type porous materials by combining pore space partition with charge reallocation. The method uses the first negatively charged pore partition ligand (2,5,8-tri-(4-pyridyl)-1,3,4,6,7,9-hexaazaphenalene, H-tph) that simultaneously enables pore partition and charge reallocation. Over two dozen anionic *pacs* materials have been made to demonstrate their excellent chemical stability and a high degree of tunability. Notably, Ni_3-bdt-tph (bdt = 1,4-benzeneditetrazolate) exhibits month-long water stability, while CoV-bdt-tph sets a new benchmark for C_2H_2 storage capacity under ambient conditions for ionic MOFs. In addition to tunable in-framework modules, we show feasibility to tune the type and concentration of extra-framework counter cations and their influence on both stability and capability to separate industrial C_3H_8/C_3H_6 and C_6H_6/C_6H_{12} mixtures.

Anionic metal-organic frameworks (MOFs), similar to zeolites with negative frameworks, represent only a minute fraction of MOFs that are typically neutral.[1] The availability of stable and tunable anionic MOFs can enable new applications in sorption,[2] ion exchange,[3] etc.[4]. Currently, few systematical strategies are available to construct and tune anionic MOFs.[5] Even in systems that can accommodate host-guest modification, the degree of tunability is limited, and the reduction in porosity and stability is often taken as a necessary tradeoff.[6] Hence the development of methods to systematically construct stable anionic MOFs with a wide degree of tunability poses a significant challenge.

The 9-connected *pacs* system has been shown to be an ultra-tunable platform.[7] Its framework formula is $[(M1)_{3-x}(M2)_x(O/OH/)(L1)_3(L2)]$, where metal trimers are linked by framework-forming L1 and pore-partitioning L2 ligands of various size and functionality. The different combinations of these modules allows *pacs* materials to be incredibly versatile, and hence, capable of setting performance records in applications.[8]

It has been shown that anionic *pacs* materials can be made from all-M^{2+} ions to give negative trimer $[(M^{2+})_3(\mu_3\text{-}OH)(COO^-)_6]^-$, whereas the inclusion of M^{3+} could turn the framework neutral or cationic.[7a, 8c, 9] Given the possibility for 3d-metals to adopt both M^{2+} and M^{3+}, only some metal types (e.g., Mg^{2+}, Zn^{2+}) could guarantee anionic trimer, which poses two major problems: stability and versatility. First, ligand-field stabilization energy plays no roles in stabilizing M—O or M—N bonds (M=Mg/Zn). Consequently, these trimers are more prone to ligand exchange (water degradation in particular). Additionally, the synthesis using all-M^{2+} trimers eliminates many benefits from other metal types or heterometal chemistry (e.g., Co-V). Thus, the metal-node-based strategy to develop anionic *pacs* dramatically limits the true potential of the *pacs* platform.

In this work, by taking advantage of highly modular features of the *pacs* platform where the charge property of each module can be independently engineered and allocated, we envision a method for creating anionic MOFs by shifting negative charges from hydrolysis-prone metal nodes to chemically resistant core of pore partition ligands (Scheme 1). This method permits much more freedom in metal choices and also makes it possible to increase the metal-ligand bond strength by harnessing desirable properties of diverse metal types beyond d^0 and d^{10} M^{2+} ions.

Here, we introduce the first negatively charged organic pore partition ligand, a tripyridyl linker with an acidic central N-rich hexaazaphenalene ring (hap) (Figure 1). With the tritopic linker bearing the negative charge, we no longer need to rely on inorganic nodes for generating negative charge. We show that module 1 could accommodate anionic Mg_3, Zn_3 trimers, as well as anionic or neutral Co_3, Ni_3, Mg_xV_y, Co_xV_y, Co_xFe_y, and Ni_xFe_y trimers. Additionally, this tripyridyl linker is compatible with

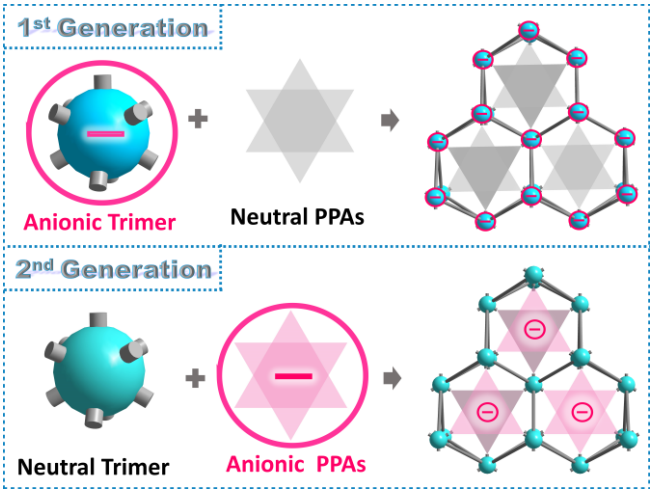

Scheme 1. Design of robust anionic *pacs* through simultaneous pore space partition and charge shifting from 9-connected inorganic node to PPA. PPA = Pore Partition Agent.

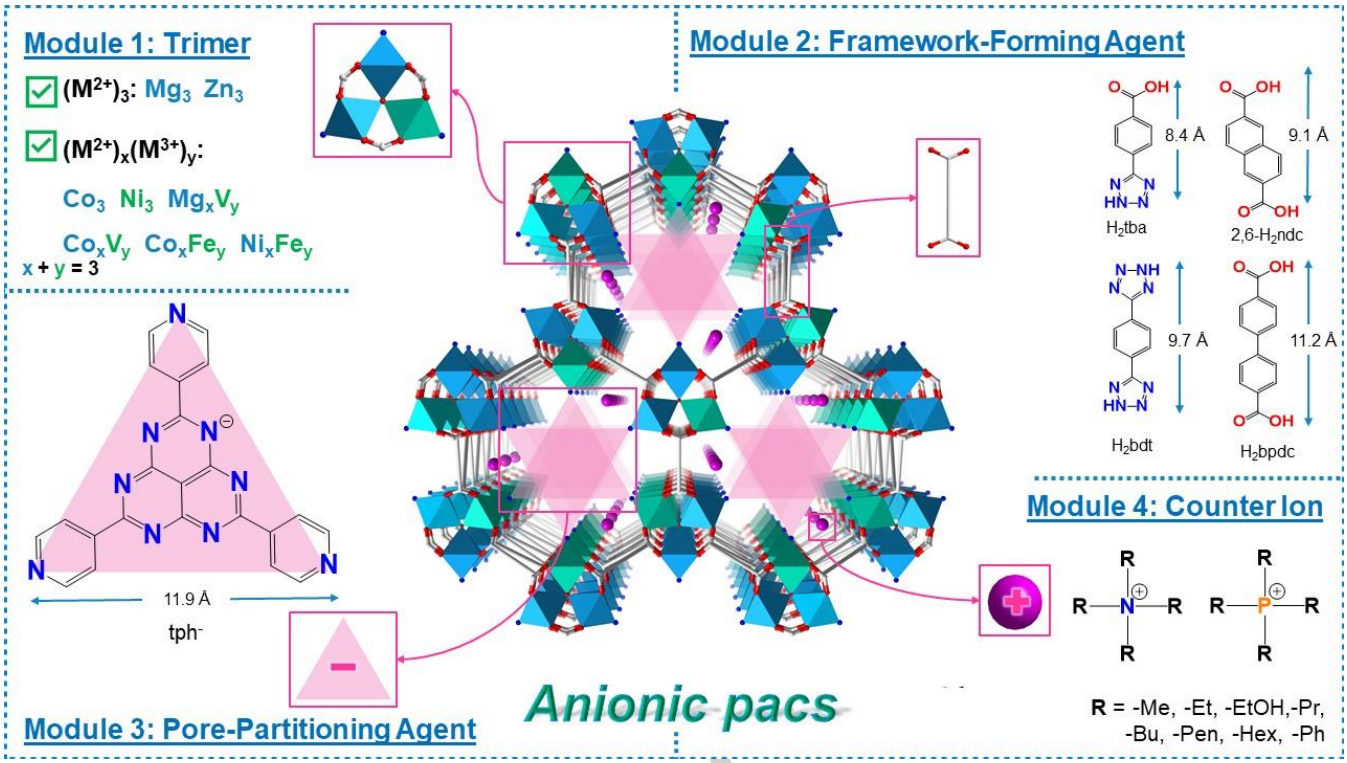

Figure 1. Design of tph-based anionic *pacs* frameworks with different modules. Module 1: Metal composition in neutral and anionic trimers. Module 2: 4-(1H-tetrazol-5-yl)benzoic acid (H_2tba), 1,4-benzeneditetrazole (H_2bdt), 2,6-naphthalenedicarboxylic acid (2,6-H_2ndc), 4,4'-biphenyldicarboxylic acid (H_2bpdc). Module 3: 2,5,8-tri-(4-pyridyl)-1,3,4,6,7,9-hexaazaphenalene (H-tph). Module 4: tetraethylammonium chloride (Et_4NCl), tetrapropylammonium chloride (Pr_4NCl), tetrabutylammonium chloride (Bu_4NCl), tetrapentylammonium chloride (Pen_4NCl), tetrahexylammonium chloride (Hex_4NCl), (2-hydroxyethyl)trimethylammonium chloride (htmNCl), bis(2-hydroxyethyl)dimethylammonium chloride (dhdmNCl), tetraphenylphosphonium bromide (Ph_4PBr).

module 2 (L1 ligands) of a wide range of dimensions and functional groups. Four representative L1 ligands are demonstrated here that contain two carboxylate groups (2,6-H_2ndc, H_2bpdc), two azolate groups (H_2bdt), as well as mixed carboxylate-azolate groups (H_2tba), respectively.

Central to our strategy is the presence of six nitrogens at the core of the pore-partitioning ligand (the hap ring) to resonance-stabilize the anionic site. We took advantage of this property to control the next variable of the *pacs* system: the counter ions (module 4, guest ions G1). A simple synthetic procedure has been developed to simultaneously construct anionic *pacs* and substitute hap's charge-balancing ion with quaternary ammonium or phosphonium ions that contain hydroxy, aliphatic and aromatic groups.

A series of isoreticular structures have been synthesized from the permutation of three modules (trimer-L1-G1), each with a large library of selection. As such, the frameworks contain aperture of varied size, shape and functionality. These examples show great potential to develop robust and versatile anionic MOFs with optimized host-guest recognition for selective gas and vapor sorption.

Crystal structures of tph-based *pacs* were first determined by single-crystal X-ray diffraction (SXRD).[10] Powder X-ray diffraction (PXRD) then confirmed phase purity of L1-tph based *pacs* of different metal and counterion sources. The powder patterns of as-synthesized samples match well with those simulated from single crystal data (Figure S1-S6).

The M^{2+} to M^{3+} ratios of heterometal phases are supported by energy dispersive spectroscopy (EDS) analysis and summarized in Figure S21. For all heterometal phases, the ratio of M^{2+} to M^{3+} is greater than 1. ^{1}HNMR was then employed to calculate the ratio of the added organic cation to the formula unit, as summarized in Table S2 which also shows this ratio could be tuned. For instance, the addition of 0.2 mmol Bu_4NCl resulted in tph:Bu_4 ratio of 2:1 in **Co_2V-26ndc-tph**, whereas a 15.0 mmol addition of Bu_4NCl resulted in tph:Bu_4 ratio of 1:1.

Hydrolytic stability is an important requisite for applications.[11] Yet the number of water-stable anionic MOFs is limited (Table S7). This work also shows that the anionic metal-node resulted in hydrolytically less stable porous materials. For example, **Mg_3-26ndc-tph** from this work could not maintain water stability for 5 minutes. In comparison, **Co_2V-26ndc-tph** is highly stable in water for at least 3 days (Figure 2a). Co_2V-26ndc-tph also maintains chemical stability within pH range 3-11 for at least 24 hours (Figure S8). This illustrates the potential of the charge-reallocation strategy for developing a large family of anionic *pacs* materials.

The hydrolytic stability of Co_2V-26ndc-tph could further be enhanced through choice of counter cation. As shown in Figure S7, **Co_2V-26ndc-tph** synthesized with hydroxy-functionalized, aliphatic, or aromatic-based counter cations all maintain water stability for at least 24 hours. The *pacs* material prepared from the addition of 10 mmol Ph_4PBr extends stability to at least 21 days, and pH range 3-11 for 14 days (Figure S8). This is likely due to the presence of bulky hydrophobic Ph_4P^+ counterions that impede H_2O attack on metal sites and thus allow the material to maintain chemical stability over a much longer period.

In addition to high chemical stability observed in carboxylate-based *pacs*, we also witnessed remarkable properties with azolate-based *pacs* materials. In particular, **Ni_3-bdt-tph** reported

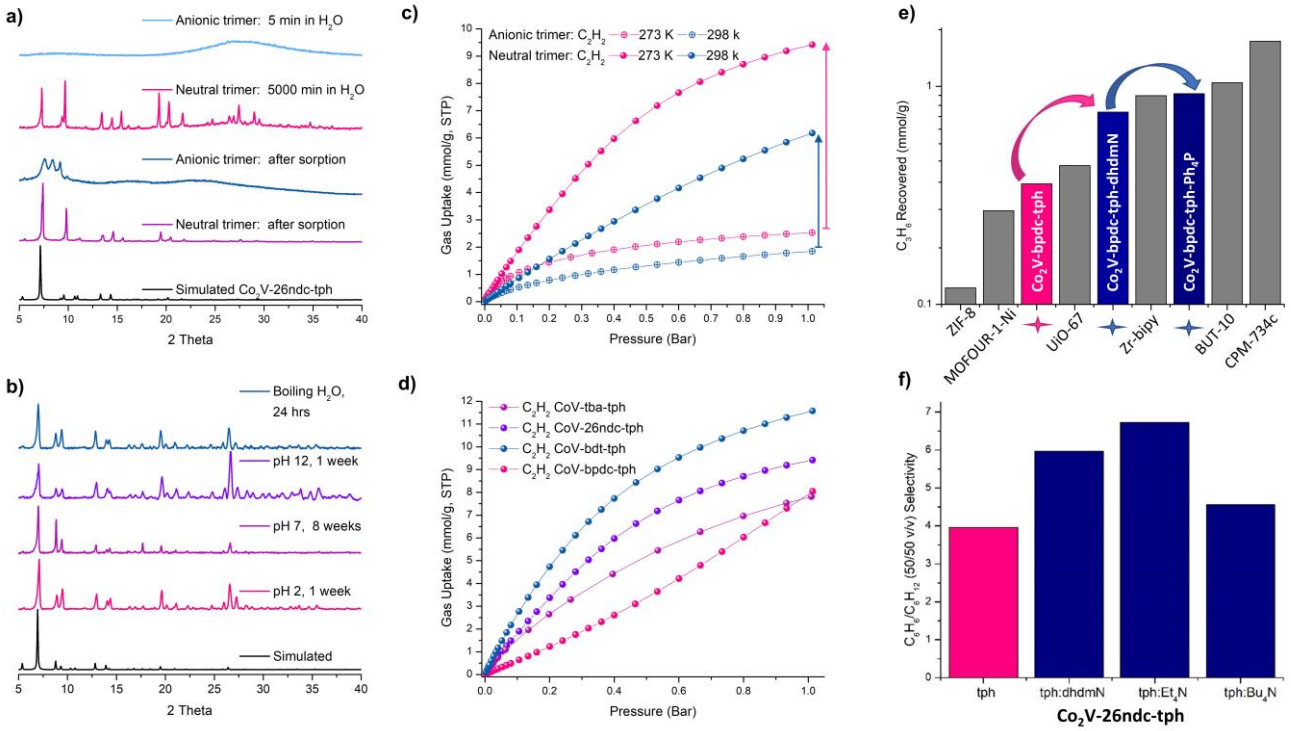

Figure 2. PXRD patterns and C_2H_2 gas sorptions, C_3H_8/C_3H_6 sepration potentials and C_6H_6/C_6H_{12} selectivities of anionic pacs. (a) Comparison of stability (in water and after gas sorption) of *pacs* made from anionic trimer (Mg_3) versus neutral trimer (Co_2V). (b) Hydrolytic stability **Ni_3-bdt-tph** in different pH and temperature conditions. (c) Comparison of C_2H_2 uptakes at 273 K and 298 K between *pacs* constructed from anionic versus neutral trimer. (d) C_2H_2 uptakes at 273K of CoV-tph-based pacs with varying L1 linkers. (e) Potentially recoverable C_3H_6 from a C_3H_8/C_3H_6 50:50 separation at 298 K for Co_2V-bpdc-tph based *pacs*. (f) C_6H_6/C_6H_{12} selectivity of Co_2V-26ndc-tph based *pacs*.

here maintains water stability for at least 2 months and stability in pH 2-12 for at least 7 days. The material also shows modest stability of 24 hours in refluxing H_2O (Figure 2b). Such high chemical stability achieved with tph ligands is comparable to benchmark anionic materials (Table S7).

Acetylene, ethylene, and propylene are all important raw organic building blocks whose storage and separation poses great challenges to many industrial sectors. For instance, the safe storage and transportation of explosive acetylene (C_2H_2) requires large cylinders pressurized below 2 bar or filled with stabilizers, which compromises purity and accrues high cost. Several benchmark materials with desirable features such as micro-pore, open-metal sites, and functional linkers have shown promising C_2H_2 storage capacity at ambient temperature and pressure.[12] The anionic *pacs* reported here presents an additional level of tunability (through counter cation) to further enhance interactions with these small gas molecules.

The formation the anionic Mn_3-26ndc-tpp (SNNU-28(Mn), tpp = 2,4,6-tri(4-pyridinyl)-1- pyridine), however, shows negligible C_2H_2 uptake, due to framework instability.[7a] Similarly, the anionic **Mg_3-26ndc-tph** reported here exhibits small uptakes of 2.52 and 1.84 mmol/g at 1 bar, 273 K and 298 K, respectively (Figure 2c). PXRD of the material after one gas sorption cycle shows unidentifiable phase change. (Figure 2a). In SNNU-28(Mn) where PPA is neutral, the substitution of Mn^{2+} with Mg^{2+} or Zn^{2+} would unlikely improve stability whereas other metals or metal combinations could likely form neutral or cationic frameworks. Here, shifting of the negative charge from metal cluster to tph linker allows us to incorporate a much wider range of metal sources into anionic *pacs*. As a result, the construction of **Co_2V-26ndc-tph**, results in C_2H_2 uptakes of 9.4 mmol/g and 6.2 mmol/g at 1 bar, 273 K and 298 K, respectively. This is a dramatic boost, from the 1st generation of unstable anionic *pacs* materials. After repeated gas sorption-desorption cycles, PXRD shows Co_2V-26ndc-tph still retains high crystallinity (Figure 2a).

With the success of **Co_2V-26ndc-tph**, we then systematically study the general porosity, C2, C3 uptake trends, to tailor specific anionic tph-pacs to the needs of different applications. As shown in Figures S24-25, all anionic *pacs* reported here show type-I N_2 adsorption isotherm. The N_2 uptake increases with elongation of L1 linkers and decreases with addition of enlarged counter ions. The surface areas and pore volumes of these materials are within expected range, based on other reported *pacs*, suggesting that they are well activated. After confirming porosity of anionic *pacs*, we then studied the adsorptions of C_2H_2, C_2H_4, C_2H_6, C_3H_6, C_3H_8 at 273 and 298 K for tph-based *pacs* with different L1 lengths. Table S3 summarizes the uptakes at 1 bar, 273 and 298 K, and isosteric heat of adsorption.

Interestingly, the C_2H_2 uptake trend at 273 K follows $bpdc^{2-}$ < tba^{2-} < $26ndc^{2-}$ < bdt^{2-}(Figure 2d). Generally, with enlarged framework having extra-large volume, host-guest interaction is dramatically diminished, thus resulting in poor uptake. Since **Co_2V-bpdc-tph** framework is too large, and thus exhibits poor uptake, **CoV-bdt-tph**, with the next largest surface area and pore volume, exhibits the highest C_2H_2 uptakes of 11.6 and 8.23 mmol/g at 273 K and 298 K, respectively. In fact, these values are also higher than the best performing ionic MOF materials NBU-8 (10.5, 8.15)[13], FJU-90a (9.64, 8.04)[8d], SNNU-60 (6.94, 5.53)[14]. C_2H_4 and C_2H_6 uptakes for CoV-bdt-tph are also the highest among all tph-pacs materials. Thus, the bdt-tph pacs combination offers the most ideal pore aperture and functionalities for optimal uptakes of small C2 molecules.

With larger C3 molecules, the elongated L1 linkers provides larger pore volume for higher uptake. **Co_2V-bpdc-tph** exhibits C_3H_6 and C_3H_8 uptakes of 12.9 and 11.8 mmol/g at 273 K, and 11.5 and 10.7 mmol/g at 298 K. While the C3 uptake capacities are among the top-three MOF materials,[15] the uptake difference between these two molecules is modest. We sought to introduce additional hydroxyl groups in organic cations to boost O---H interactions. Compared to Co_2V-bpdc-tph that could potentially recover 0.357 mmol/g C_3H_6 from C_3H_8/C_3H_6 1:1 mixture at 1 bar, 298 K, the incorporation of 0.5 dhdmN+ per formula unit resulted in 0.925 mmol/g of potentially recoverable C_3H_6 (Figure 2e). This is higher than ZIF-8 (0.119)[16], MOFOUR-1-Ni (0.269)[17], UiO-67 (.433)[18], but slightly lower than BUT-10 (1.04)[18] and CPM-734c (1.61)[8e].

Cyclohexane (C_6H_{12}) is a crucial intermediate in the petrochemical industry. However, the C_6H_{12} production results in benzene/cyclohexane mixtures that must undergo energy-intensive purifications. Porous materials provide a promising platform for C_6H_6/C_6H_{12} separation. (Table S12). Herein, we present the first case study on utilizing aliphatic organic cation to enhance C_6H_6/C_6H_{12} selectivity.

With **Co_2V-26ndc-tph** as the parent framework, we chose to incorporate Et_4N^+, Bu_4N^+ and $dhdmN^+$. Co_2V-26ndc-tph adsorbs 3.6 and 0.9 C_6H_6 and C_6H_{12} molecules per formula unit (mpf), respectively. With the substitution of 0.5 Bu_4N^+ mpf, the uptake of C_6H_6 increases to 4.8, while C_6H_{12} stayed the same. Further increase of Bu_4N^+ to 1 mpf resulted in 5% decrease of C_6H_6 but 20% decrease for C_6H_{12}. We speculate that while alkyl chain enhances π-H with C_6H_6, slight H-H repulsion with C_6H_{12} is observed when pore volume has higher concentration of Bu_4N^+. Interestingly, the shortening of the alkyl length to Et_4N did not increase C_6H_{12} uptake. The addition of 0.4 Et_4N mpf resulted in an increase of C_6H_6 to 5.8 while keeping C_6H_{12} at 0.9 mpf. The addition of two OH groups into $dhdmN^+$, slightly increased the concentration of C_6H_{12} to 1 mpf, likely through electronegative-H interaction. This shows that length, functionality, and concentration of cations all contribute to enhancing C_6H_6/C_6H_{12} selectivity (Figure 2f).

In conclusion, we demonstrated the effectiveness of employing a novel pore-partitioning linker to construct a series of anionic MOFs with highly tunable pore metrics and functionalities. We believe that this material design and synthesis strategy will lead to useful anionic MOFs for a large range of applications.

Acknowledgements. This work is supported by the U.S. Department of Energy, Office of Basic Energy Sciences, Materials Sciences and Engineering Division under Award No. DE-SC0010596 (P.F.).

Keywords: stability • anionic • MOFs • gas sorption

[1] S.-N. Zhao, Y. Zhang, S.-Y. Song, H.-J. Zhang, *Coord. Chem. Rev.* **2019**, *398*, 113007.

[2] a) G. Chang, M. Huang, Y. Su, H. Xing, B. Su, Z. Zhang, Q. Yang, Y. Yang, Q. Ren, Z. Bao, B. Chen, *Chem. Commun.* **2015**, *51*, 2859-2862; b) L. Zhang, K. Jiang, L. Yang, L. Li, E. Hu, L. Yang, K. Shao, H. Xing, Y. Cui, Y. Yang, B. Li, B. Chen, G. Qian, *Angew. Chem., Int. Ed.* **2021**, *60*, 15995-16002; c) S. Yang, X. Lin, A. J. Blake, G. S. Walker, P. Hubberstey, N. R. Champness, M. Schröder, *Nat. Chem.* **2009**, *1*, 487-493.

[3] a) P. Li, N. A. Vermeulen, X. Gong, C. D. Malliakas, J. F. Stoddart, J. T. Hupp, O. K. Farha, *Angew. Chem. Int. Ed. Engl.* **2016**, *55*, 10358-10362; b) X. Liu, Z. Xiao, J. Xu, W. Xu, P. Sang, L. Zhao, H. Zhu, D. Sun, W. Guo, *J. Mater. Chem. A* **2016**, *4*, 13844-13851.

[4] a) F. Yang, G. Xu, Y. Dou, B. Wang, H. Zhang, H. Wu, W. Zhou, J.-R. Li, B. Chen, *Nature Energy* **2017**, *2*, 877-883; b) S.-S. Liu, Z. Han, J.-S. Yang, S.-Z. Huang, X.-Y. Dong, S.-Q. Zang, *Inorg. Chem.* **2020**, *59*, 396-402; c) W. J. Phang, H. Jo, W. R. Lee, J. H. Song, K. Yoo, B. Kim, C. S. Hong, *Angew. Chem. Int. Ed. Engl.* **2015**, *54*, 5142-5146; d) M. Sadakiyo, T. Yamada, H. Kitagawa, *J. Am. Chem. Soc.* **2014**, *136*, 13166-13169; e) S. S. Nagarkar, S. M. Unni, A. Sharma, S. Kurungot, S. K. Ghosh, *Angew. Chem. Int. Ed.* **2014**, *53*, 2638-2642; f) J. M. Taylor, K. W. Dawson, G. K. H. Shimizu, *J. Am. Chem. Soc.* **2013**, *135*, 1193-1196; g) J. Tian, L. V. Saraf, B. Schwenzer, S. M. Taylor, E. K. Brechin, J. Liu, S. J. Dalgarno, P. K. Thallapally, *J. Am. Chem. Soc.* **2012**, *134*, 9581-9584; h) G.-W. Xu, Y.-P. Wu, W.-W. Dong, J. Zhao, X.-Q. Wu, D.-S. Li, Q. Zhang, *Small* **2017**, *13*, 1602996.

[5] a) S.-T. Zheng, J. T. Bu, Y. Li, T. Wu, F. Zuo, P. Feng, X. Bu, *J. Am. Chem. Soc.* **2010**, *132*, 17062-17064; b) J. An, C. M. Shade, D. A. Chengelis-Czegan, S. Petoud, N. L. Rosi, *J. Am. Chem. Soc.* **2011**, *133*, 1220-1223; c) Y. Liu, G. Li, X. Li, Y. Cui, *Angew. Chem. Int. Ed.* **2007**, *46*, 6301-6304.

[6] a) D.-X. Xue, A. J. Cairns, Y. Belmabkhout, L. Wojtas, Y. Liu, M. H. Alkordi, M. Eddaoudi, *J. Am. Chem. Soc.* **2013**, *135*, 7660-7667; b) S. Chen, J. Zhang, T. Wu, P. Feng, X. Bu, *J. Am. Chem. Soc.* **2009**, *131*, 16027-16029; c) M. Sadakiyo, H. Ōkawa, A. Shigematsu, M. Ohba, T. Yamada, H. Kitagawa, *J. Am. Chem. Soc.* **2012**, *134*, 5472-5475; d) D.-X. Xue, Y. Belmabkhout, O. Shekhah, H. Jiang, K. Adil, A. J. Cairns, M. Eddaoudi, *J. Am. Chem. Soc.* **2015**, *137*, 5034-5040; e) D. Alezi, A. M. P. Peedikakkal, Ł. J. Weseliński, V. Guillerm, Y. Belmabkhout, A. J. Cairns, Z. Chen, Ł. Wojtas, M. Eddaoudi, *J. Am. Chem. Soc.* **2015**, *137*, 5421-5430.

[7] a) Y. Y. Xue, X. Y. Bai, J. Zhang, Y. Wang, S. N. Li, Y. C. Jiang, M. C. Hu, Q. G. Zhai, *Angew. Chem. Int. Ed. Engl.* **2021**, *60*, 10122-10128; b) G. Brunet, K. Robeyns, R. P. S. Huynh, J. B. Lin, S. P. Collins, G. A. Facey, G. K. H. Shimizu, T. K. Woo, M. Murugesu, *ACS Appl Mater Interfaces* **2019**, *11*, 3181-3188; c) H.-J. Ding, Y. Zhang, X. Wang, Q.-Y. Lin, S.-M. Zhang, M.-H. Yu, Z. Chang, X.-H. Bu, *Inorg. Chem.* **2021**, *60*, 5122-5130; d) J.-N. Lu, J. Liu, L.-Z. Dong, S.-L. Li, Y.-H. Kan, Y.-Q. Lan, *Chem. Eur. J.* **2019**, *25*, 15830-15836; e) Y.-S. Wei, M. Zhang, P.-Q. Liao, R.-B. Lin, T.-Y. Li, G. Shao, J.-P. Zhang, X.-M. Chen, *Nat. Commun* **2015**, *6*, 8348.

[8] a) H. Yang, Y. Wang, R. Krishna, X. Jia, Y. Wang, A. N. Hong, C. Dang, H. E. Castillo, X. Bu, P. Feng, *Journal of the American Chemical Society* **2020**, *142*, 2222-2227; b) Y. Wang, X. Jia, H. Yang, Y. Wang, X. Chen, A. N. Hong, J. Li, X. Bu, P. Feng, *Angew. Chem. Int. Ed.* **2020**, *59*, 19027-19030; c) X. Zhao, X. Bu, E. T. Nguyen, Q.-G. Zhai, C. Mao, P. Feng, *J. Am. Chem. Soc.* **2016**, *138*, 15102-15105; d) Y. Ye, Z. Ma, R. B. Lin, R. Krishna, W. Zhou, Q. Lin, Z. Zhang, S. Xiang, B. Chen, *J. Am. Chem. Soc.* **2019**, *141*, 4130-4136; e) A. N. Hong, H. Yang, T. Li, Y. Wang, Y. Wang, X. Jia, A. Zhou, E. Kusumoputro, J. Li, X. Bu, P. Feng, *ACS Appl. Mater. Interfaces* **2021**, *13*, 52160-52166; f) Y. Wang, X. Zhao, H. Yang, X. Bu, Y. Wang, X. Jia, J. Li, P. Feng, *Angew. Chem. Int. Ed.* **2019**, *58*, 6316-6320; g) Y.-S. Wei, M. Zhang, M. Kitta, Z. Liu, S. Horike, Q. Xu, *J. Am. Chem. Soc.* **2019**, *141*, 7906-7916.

[9] H.-R. Yang, W.-Y. Chen, D.-M. Chen, Y.-P. Zheng, S.-M. Fang, *J. Solid State Chem.* **2020**, *291*, 121658.

[10] The CCDC depository numbers of Co3-tba-tph, CoV-26ndc-tph, CoV-bdt-tph, and CoV-bpdc-tph are 2124127, 2124128, 2124129, and 2124130, resepectively.

[11] a) M. Ding, X. Cai, H.-L. Jiang, *Chem. Sci.* **2019**, *10*, 10209-10230; b) L. N. McHugh, M. J. McPherson, L. J. McCormick, S. A. Morris, P. S. Wheatley, S. J. Teat, D. McKay, D. M. Dawson, C. E. F. Sansome, S. E. Ashbrook, C. A. Stone, M. W. Smith, R. E. Morris, *Nat. Chem.* **2018**, *10*, 1096-1102.

[12] a) Z. Di, C. Liu, J. Pang, C. Chen, F. Hu, D. Yuan, M. Wu, M. Hong, *Angew. Chem. Int. Ed. Engl.* **2021**; b) F. Moreau, I. da Silva, N. H. Al Smail, T. L. Easun, M. Savage, H. G. W. Godfrey, S. F. Parker, P. Manuel, S. Yang, M. Schröder, *Nat. Commun* **2017**, *8*, 14085; c) J. Pang, F. Jiang, M. Wu, C. Liu, K. Su, W. Lu, D. Yuan, M. Hong, *Nat. Commun* **2015**, *6*, 7575.

[13] Q. Li, N. Wu, J. Li, D. Wu, *Inorg. Chem.* **2020**, *59*, 13005-13008.

[14] J.-W. Zhang, M.-C. Hu, S.-N. Li, Y.-C. Jiang, Q.-G. Zhai, *Chem. Eur. J.* **2017**, *23*, 6693-6700.

[15] a) P. Huang, C. Chen, Z. Hong, J. Pang, M. Wu, F. Jiang, M. Hong, *Inorg. Chem.* **2019**, *58*, 11983-11987; b) W. Fan, X. Wang, X. Zhang, X. Liu, Y. Wang, Z. Kang, F. Dai, B. Xu, R. Wang, D. Sun, *ACS Cent. Sci.* **2019**, *5*, 1261-1268.

[16] U. Böhme, B. Barth, C. Paula, A. Kuhnt, W. Schwieger, A. Mundstock, J. Caro, M. Hartmann, *Langmuir* **2013**, *29*, 8592-8600.

[17] L. Yang, X. Cui, Q. Ding, Q. Wang, A. Jin, L. Ge, H. Xing, *ACS Appl. Mater. Interfaces* **2019**, *12*, 2525–2530.

[18] C. He, Y. Wang, Y. Chen, X. Wang, J. Yang, L. Li, J. Li, *Chem. Eng. J.* **2021**, *403*, 126428.

Entry for the Table of Contents

Charge Shifting via Pore Partition: a nine-nitrogen ligand simultaneously enables pore-space partition (via three N's) and charge reallocation (via six N's), thereby paving the way for multi-modular assembly of a huge family of tunable anionic porous materials with much enhanced chemical stability and selective gas and vapor sorption.